Psilocybin-Induced Behavioral and Cellular Effects

Albert Dong[1], Yi Han[2], Zheng Xu[2], Xiaojie Huang[2], Oliver M. Schluter[2]

1. Sewickley Academy, Sewickley, PA
2. Department of Neuroscience, University of Pittsburgh, PA

Abstract

Psilocybin, a prominent psychedelic, recently emerged as a potential therapeutic agent for treating psychiatric disorders, yet the molecular and cellular mechanisms driving its effects remain poorly understood. To address these knowledge gaps, we focused on the nucleus accumbens (NAc), a forebrain region that regulates reward, motivation, and emotion. Using DeepLabCut, a deep neural-network toolbox, we revealed that administration of psilocybin (3 mg/kg) induced a rapid behavioral inhibition in mouse locomotion, peaking at ~20 min and resolving by ~60 min post-psilocybin treatment. By contrast, at the cellular level we uncovered a complex, prolonged c-Fos expression profile. We found that the density of c-Fos-expressing neurons in the NAc peaked at 6 h, while the density of c-Fos-expressing non-neurons peaked earlier at 1.5 h post-psilocybin treatment. These temporal profiles suggest that, as an immediate early gene and transcription factor, c-Fos may induce prolonged functional changes of NAc neurons and non-neurons through transcriptional regulation. Finally, to probe for endogenous receptors that may mediate the psilocybin effects, we focused on 5-HT2A and 5-HT2B serotonin receptors. We found that inhibition of 5-HT2A receptors (Volinanserin, 0.5 mg/kg) selectively reduced psilocybin-induced c-Fos expression in neurons, whereas inhibition of 5-HT2B receptors (RS 127445, 0.5 mg/kg) reduced psilocybin-induced c-Fos expression in both neuronal and non-neuronal cells. These findings challenge the neuron-centric view of psychedelic action, identifying 5-HT2B receptors and non-neuronal cells as potential key players in the regulation of circuits underlying mood-related disorders.

Introduction

After decades of limited scientific attention, psychedelic compounds are now gaining renewed interest for their profound affective effects and, more importantly, their therapeutic potential in treating psychiatric disorders[1]. A growing body of clinical work suggests that even a single administration of psychedelics can produce rapid and lasting improvements of a broad range of psychiatric conditions, including depression, anxiety, substance use disorders, and post-traumatic stress disorder[2,3]. These findings raise the possibility that psychedelics represent a new class of psychiatric therapeutics[4,5]. Psilocybin, one of the most studied psychedelics, is a prodrug and rapidly converted to psilocin after ingestion[5]. Psilocin binds to serotonin receptors in the brain, where it alters the processing of sensory and visceral information related to emotion and motivation[6]. Despite the prominent behavioral effects, it remains elusive how psilocybin administration affects emotional and motivational responses.

Among several candidate brain regions, we focused on the nucleus accumbens (NAc), a hub in the brain reward circuit that regulates emotional and motivational responses under both physiological and pathophysiological conditions[7,8]. In the NAc, medium spiny neurons (MSNs) are the principal neurons, constituting >90% of the total neuronal population[9]. NAc MSNs integrate and prioritize cortical and subcortical inputs that carry emotional and motivational information for behavioral outputs[10]. In the NAc, there are also non-neuronal cells, mainly astroglia, which outnumber MSNs[11,12]. Astroglia and other non-neuronal cells not only support but also actively regulate the operation of adjacent MSNs[13], but whether these non-neuronal cells respond to psilocybin remains largely unclear. To gain insight into the collective effect of psilocybin on the NAc function, our study examined both neuronal and non-neuronal cells in parallel.

Prior studies have established 5-HT2A as the canonical serotonin receptor that mediates the psychohallucigenic effects of psilocybin[5,14]. However, 5-HT2B, which exhibits a higher

binding affinity to psilocin than 5-HT2A[15,16], has been critically implicated in mood regulation[17]. These findings led us to examine both 5-HT2A and 5-HT2B in parallel.

In this study, we tested the hypothesis that psilocybin activates both neurons and non-neurons in the nucleus accumbens, which are differentially mediated by 5-HT2A vs 5-HT2B receptors. First, we used DeepLabCut to reveal an acute inhibition of locomotor activities in mice following psilocybin administration (3 mg/kg, i.p.). Next, we used immunohistochemistry to characterize the temporal profile of psilocybin-induced expression of c-Fos, an immediate early gene that reports strong cellular activation, in both neurons and non-neurons in the NAc. Specifically, in mice after psilocybin administration (3 mg/kg, *i.p.*), the density of c-Fos-expressing neurons, indicated by c-Fos and NeuN co-labeling, increased gradually and peaked at 6 h post-administration. By contrast, the density of c-Fos-expressing non-neuronal cells peaked at 1.5 h, suggesting distinct temporal dynamics between different cell populations. Finally, we used pharmacology to differentiate the role of 5-HT2A and 5-HT2B receptors in mediating psilocybin-induced c-Fos expression. We found that pretreatment with 5-HT2A antagonist (Volinanserin, 0.5 mg/kg, *i.p.*) selectively reduced psilocybin-induced neuronal activation, while 5-HT2B blockade (RS 127445, 0.5 mg/kg, *i.p.*) reduced both neuronal and non-neuronal activation. These results suggest that psilocybin-induced activation of non-neurons is selectively mediated by 5-HT2B receptors, and there is potential cross-talk downstream of 5-HT2B between neurons and non-neurons. These findings suggest that psilocybin engages multiple serotonergic signaling pathways to induce prolonged cellular activation in both neurons and non-neurons, which collectively affect the emotional and motivational state.

Methods

Animals

Male C57BL/6J mice at the age of 9 weeks (purchased from Jackson Laboratories) were used for all experiments. Mice were housed under standard laboratory conditions (lights on from 07:00 to 19:00; temperature at 23 ± 2 °C; humidity at 55–60%) with ad libitum access to food pellets and water. All experimental procedures complied with animal care standards by the National Institute of Health and under the IACUC protocol proved by the University of Pittsburgh.

Psilocybin administration

Psilocybin (obtained from Sigma-Aldrich) was diluted with 0.9% sterile saline and administered to each mouse via *i.p.* injection at 3 mg/kg.

Slice preparation

Mice were deeply anesthetized with intraperitoneal injection of ketamine and xylazine (50/5 mg/kg) and transcardially flushed with 20 ml of 0.01 M cold phosphate-buffered saline (PBS, pH = 7.4), followed by 10 ml of PBS containing 4% paraformaldehyde. Immediately after perfusion, the brains were carefully removed and post-fixed in 4% paraformaldehyde at 4 °C for 24 h. The brains were then dehydrated in 20% sucrose-PBS solution for 24 h, followed by 30% sucrose for 24 h. Coronal sections (30 μm) were prepared using a cryostat microtome (Thermo Scientific CryoStar NX50, Germany).

Immunohistochemistry

Brain sections were rinsed in PBS three times for 5 min, followed by incubation in 1% normal goat serum in PBS containing 0.4% Triton X-100 (TBS) for 45 min at room temperature to block nonspecific reactions. The sections were then incubated overnight with the primary antibodies diluted in TBS at 4 °C in a shaker. The primary antibodies included rabbit anti-c-Fos (1:1000, Cell Signaling Technology, 2250) and mouse anti-NeuN (1:500, Cell Signaling Technology, 94403). Brain sections were then washed three times in TBS for 10 min and incubated for 2 h

with the corresponding fluorophore-conjugated secondary antibody in TBS. The secondary antibodies included anti-rabbit Alexa 488 (1:500, Thermo Fisher Scientific, A21206) and anti-mouse Alexa 594 (1:300, Thermo Fisher Scientific, A21203). Brain sections were washed twice in TBS for 10 min each time and in PBS for 10 min at room temperature, then mounted using DAPI-containing mounting media (abcam #ab104139) and dried overnight before microscopy.

Confocal microscopy

Sections were imaged using a Leica TCS SP5 confocal microscope controlled by Leica Application Suite software. Images were acquired with a 5x air objective or 10x water-immersion objective.

Behavioral analysis

Behavioral tracking was performed using DeepLabCut. DeepLabCut relies on convolutional neural networks to learn the mapping between image pixels and user-defined body part locations. We used a ResNet-50 backbone as the feature extractor. ResNet-50 is a 50-layer residual network architecture that uses “skip connections” to allow information to bypass intermediate layers, improving accuracy in pose estimation. The network was trained using 90 manually labeled frames to detect the following body points: head, neck, ears, middle back, tail root, and mid-tail. Each full pass through the training dataset is termed an epoch. The networks were trained for 200 epochs to reach >90% accuracy. After training, all videos were analyzed to generate x, y coordinates and likelihood values for each labeled body part. Pose estimates underwent likelihood-based filtering to reduce jitter and remove low-confidence predictions. These outputs were used for following behavioral analyses.

Frame-to-frame displacement (in pixels) of the back_mid point was used to quantify movement. These displacements were summed for total distance traveled. For per-minute locomotor metrics, speed values were averaged within each minute using only valid frames. Specifically, average speed per minute was calculated using the total displacement in valid frames in 1 minute divided by the total number of valid frames in that minute.

Fiji (ImageJ) Data Quantification

All image analyses were performed blind to treatment conditions. Images were first smoothed and despeckled to reduce background noise. Intensity thresholds were then applied to generate binary masks, and holes within labeled nuclei were filled to ensure accurate representation of complete cells. Watershed segmentation was applied to both c-Fos and NeuN channels to separate closely adjacent cells. Cell counts were obtained using ImageJ's particle analysis with size parameters set from 35 μm² to 200 μm² and circularity threshold set at 0.75 across conditions to ensure unbiased quantification.

Statistical analyses

Two-way repeated-measures ANOVA: Behavioral data collected across time were analyzed using two-way repeated-measures ANOVAs with treatment (psilocybin vs control) and time as factors, which accounts for within subject correlations. When significant main effects or interactions were detected, *Sidak*'s multiple-comparisons post hoc tests were used to determine specific group differences. One-way ANOVA: For comparisons across post-treatment time points (1.5 h, 6 h, 24 h), one-way ANOVAs were performed followed by *Tukey*'s post hoc test. Two-way ANOVA; Receptor antagonist experiments were analyzed using two-way ANOVAs with treatment and antagonist condition as factors. When significant psilocybin + antagonist

interactions were found, *Tukey*'s multiple-comparisons tests were conducted to identify pairwise differences between vehicle, psilocybin, 5-HT2A antagonist, and 5-HT2B antagonist conditions.

Data Presentation

Results are shown as bar graphs or line plots generated in Prism 10 (Graphpad). Individual data points were displayed when possible to illustrate variability. Statistical significance was $*p<0.05$, $**p<0.01$, $***p<0.001$, and $****p<0.0001$. Data were presented as mean ± SEM.

Materials

Animals: Male C57BL/6J mice (9 weeks old; Jackson Laboratory).

Chemicals & Reagents: Psilocybin (Sigma-Aldrich); Volinanserin (Cayman Chemical Company); RS 127445 (Cayman Chemical Company); Ketamine-Xylazine mixture; 0.9% sterile saline (Sigma-Aldrich); PBS (0.01 M, pH 7.4) (Sigma-Aldrich); 4% paraformaldehyde; Sucrose (20% and 30%) (Sigma-Aldrich); Triton X-100; Normal goat serum; DAPI mounting medium

Primary Antibodies: Rabbit anti-c-Fos (CST #2250); Mouse anti-NeuN (CST #94403).

Secondary Antibodies: Alexa 488 anti-rabbit (Cell Signaling Technology); Alexa 594 anti-mouse (Cell Signaling Technology).

Equipment: Cryostat (Thermo CryoStar NX50); Confocal microscope (Leica TCS SP5); Microscope slides and Coverslips (Thermo Scientific adhesive).

Software: DeepLabCut (ResNet-50); ImageJ; Leica Application Suite.

Risks and Safety

This project was conducted in a certified BSL-2 laboratory under trained supervision and in compliance with institutional safety guidelines.

Paraformaldehyde (PFA) is toxic and a potential irritant. All PFA preparation and handling were performed in a chemical fume hood while wearing appropriate personal protective equipment (PPE), including gloves, lab coat, and eye protection. Contact and inhalation exposure were minimized, and waste PFA was disposed of as hazardous chemical waste according to institutional protocols.

All animal tissues and biological materials were handled using standard biosafety procedures. Biowaste was disposed of in designated biohazard containers and processed according to BSL-2 waste disposal regulations. No materials were removed from the laboratory environment.

The cryostat microtome contains a sharp blade that presents a laceration risk. Cut-resistant gloves and standard PPE were used, and blade handling followed manufacturer and laboratory safety guidelines. The blade guard was engaged when not actively sectioning.

Standard PPE (lab coat, gloves, closed-toe shoes) was worn at all times. All procedures were conducted under trained supervision, and institutional animal care and laboratory safety protocols were followed.

Results

Psilocybin inhibits locomotor activity

In humans and rodents, reduced movement represents a behaviorally overt feature accompanying psilocybin's psychedelic effects[18]. To examine this behavioral correlation in mice, we prepared a set of mice to assess their locomotor response to psilocybin administration. We initiated the procedure by acclimating the mice to the experimenter's handling for 3 days to reduce nonspecific effects. On the experimental day, we randomly assigned the mice to receive either saline or psilocybin (3 mg/kg) injection, then placed the mice in the behavioral chambers to video-record locomotor activities for 120 min (**Figure 1A**).

To analyze the videos, we employed a deep learning-embedded algorithm, DeepLabCut (DLC), and extracted the coordinates of representative mouse body parts (**Figure 1A**) every 100 ms across the entire 2 h session. We then used these coordinates to calculate the distance that the mouse traveled over the period. Using the mid back point to represent the mouse's location, we found that mice receiving saline injection traveled significantly longer cumulative distances than psilocybin-treated mice (psilocybin x time interaction: $F(118, 1416) = 21.58$, $p < 0.0001$; 38-120 min post-psilocybin versus saline, $p < 0.05$, 0.01, 0.001, or 0.0001, 2-way repeated measure ANOVA with *Sidak* post-test; **Figure 1B**). Using data from other body parts in this analysis yielded similar results (data not shown). Moreover, psilocybin reduced locomotor speed compared to saline injections (psilocybin x time interaction: $F(118, 1416) = 3.660$, $p < 0.0001$; 15-55 min post-psilocybin versus saline, $p < 0.05$, 0.01, 0.001, or 0.0001, 2-way repeated measure ANOVA with *Sidak* post-test; **Figure 1C**), suggesting that this was a pharmacological effect rather than a reaction to *i.p.* injection per se. These results suggest that psilocybin administered at the dose of 3 mg/kg acutely decreases the locomotor activity in mice.

Psilocybin increases the density of c-Fos-expressing neurons and non-neuronal cells in NAc.

C-Fos is an immediate early gene triggered by increased cellular activities, thus is widely used to define cells that respond to a specific stimulus[19]. Our primary objective of this experiment was to examine c-Fos expression in the NAc in response to psilocybin administration.

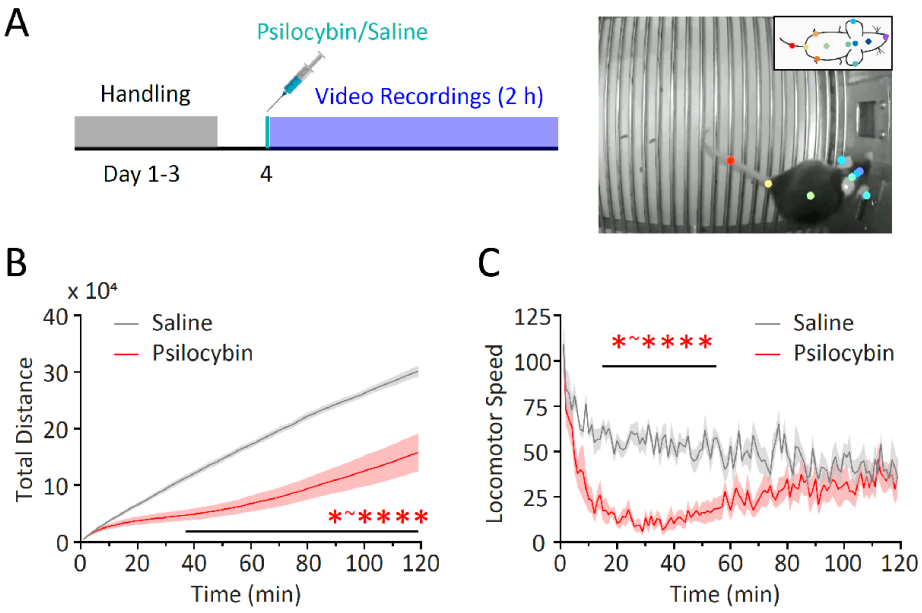

Figure 1 Psilocybin inhibits locomotor activity. **A** Experimental timeline and video tracking of mouse movements. Using DeepLabCut, we assigned virtual dots on the mouse's body parts, including the head, neck, ears, middle back, tail root, and mid-tail (*inset*), and trained the algorithm to follow these dots as the mouse was moving until the accuracy reached >90%. **B** Total distance (pixels) traveled measured by the "middle back" coordinates for the 2-h period following *i.p.* injection of saline or psilocybin (3 mg/kg). **C** Locomotor speed (pixels per frame per min) measured by the "middle back" coordinates for the 2-h period from the same groups of mice as in **B**. n=7 each, 2-way Repeated-Measure ANOVA with *Sidak*'s post hoc tests. * $p<0.05$, **** $p<0.0001$

After psilocybin administration (3 mg/kg, *i.p.*), we collected the mice brains at three time points, 1.5 h, 6 h, and 24 h post-treatment, and used mice with handling but not psilocybin treatment as baseline controls (**Figure 2A**). We then prepared brain slices for immunohistochemistry to detect c-Fos expression in individual NAc cells. While the density of c-Fos-expressing NAc cells in control mice was low, the density increased after psilocybin administration, reaching statistical significance at 6 h post-administration ($F(3, 21) = 21.42$, $p<0.0001$; baseline versus 1.5 h: $p=0.114$, 6 h: $p<0.001$, 24 h: $p=0.07$; 1-way ANOVA with *Tukey*'s post-test; **Figure 2B,C**). At all time points, most, but not all, of c-Fos+ cells also showed immunoreactivity to NeuN (% c-Fos+ cells that were NeuN+, baseline: **Figure 2D**), a neuron marker, suggesting that the majority of c-Fos+ cells were neurons.

Following psilocybin, the density of both neurons and non-neuronal (NeuN-) cells that expressed c-Fos exhibited a time-dependent increase (neurons: $F(3, 21) = 15.33$, $p<0.0001$, non-neurons: $F(3, 21) = 10.48$, $p<0.001$; 1-way ANOVA with *Tukey*'s post-test; **Figure 2D-F**).

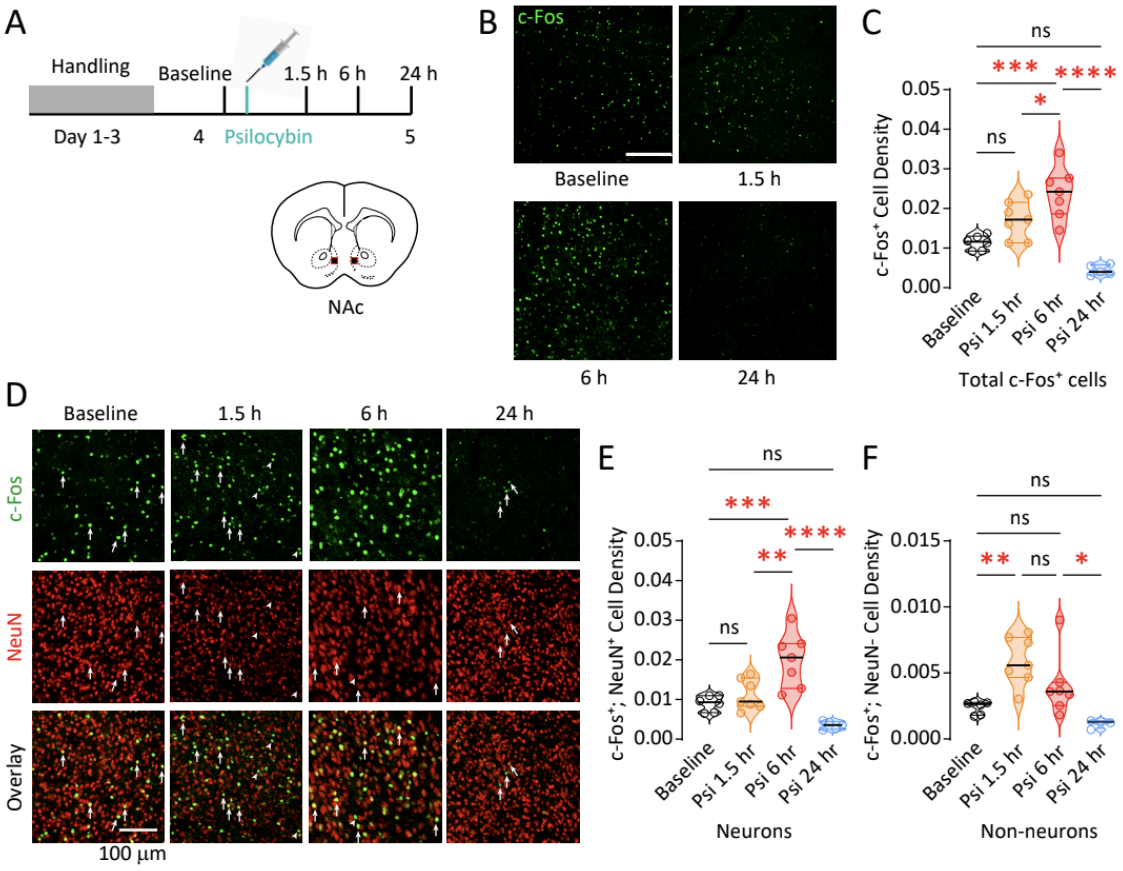

Figure 2 Psilocybin increases the density of c-Fos-expressing neurons and non-neuronal cells in NAc. **A** Experimental timeline and diagram showing a coronal section with regions of interest in the NAc (*squares*). **B** Example confocal images of NAc c-Fos immunofluorescence at baseline and three different time points following psilocybin injection. Scale bar = 200 μm. **C** Grouped data showing c-Fos+ cell density in the NAc at baseline and three different time points following psilocybin injection. **D** Example confocal images of c-Fos, NeuN, or overlaid immunofluorescence from NAc tissue at baseline and three different time points following psilocybin injection. Scale bar = 100 μm. *Arrows*: neurons, *Arrow heads*: non-neurons. **E** Grouped data showing c-Fos+ neuron (c-Fos and NeuN dual positive) density in the NAc at baseline and three different time points following psilocybin injection. **F** Grouped data showing c-Fos+ non-neuron (c-Fos+ but NeuN-) density in the NAc at baseline and three different time points following psilocybin injection. **C**,**E**,**F**, 1-way ANOVA with *Tukey*'s post hoc test. n=5-7 sections per condition. * $p<0.05$, ** $p<0.01$, *** $p<0.001$, **** $p<0.0001$, ns = not significant. psi = psilocybin

Importantly, non-neuronal cells reached the peak of c-Fos expression at 1.5 h (baseline versus 1.5 h: $p<0.01$, 6 h: $p=0.300$, 24 h: $p=0.465$; *Tukey*'s post-test; **Figure 2F**), earlier than the neuronal peak at 6 h (baseline versus 1.5 h: $p=0.789$, 6 h: $p<0.001$, 24 h: $p=0.186$; *Tukey*'s post-test; **Figure 2E**). Thus, the response of non-neuronal cells to psilocybin preceded the neuronal response. This temporal sequence raises a possibility that responses in non-neuronal cells may serve as an essential priming step for subsequent neuronal responses.

Differential contributions of serotonin 5-HT2A versus 5-HT2B receptors

To determine which serotonin receptor subtypes were involved in psilocybin-induced c-Fos expression, we examined both 5-HT2A and 5-HT2B, the two serotonin receptors that have high binding affinities to psilocin and are implicated in psilocybin-mediated psychedelic effects[16].

Forty min before psilocybin administration, we intraperitoneally injected the mice with either the 5-HT2A-selective antagonist volinanserin (0.5 mg/kg) or 5-HT2B-selective antagonist RS 127445 (0.5 mg/kg). We then collected brain tissues at 6 h post-psilocybin for c-Fos immunohistochemistry (**Figure 3A**). We observed a psilocybin x antagonist interaction effect ($F(2, 67) = 61.27$, $p<0.0001$, two-way ANOVA). Specifically, when both neuronal and

non-neuronal NAc cells were sampled together, we observed increased densities of c-Fos+ cells in vehicle injected mice after either volinanserin or RS 127445 injection, depicting the basal effects of these antagonists (vehicle versus volinanserin: $p<0.0001$, vehicle versus RS 127445: $p<0.001$; *Tukey*'s post-test; **Figure 3B-D**). Importantly, administration of either volinanserin or RS127455 attenuated the psilocybin-induced c-Fos expression (saline versus psilocybin: $p<0.0001$, psilocybin +vehicle versus +volinanserin: $p<0.0001$, psilocybin +vehicle versus +RS 127445: $p<0.0001$; *Tukey*'s post-test; **Figure 3B-D**), suggesting that both 5-HT2A and 5-HT2B are required for this psilocybin effect.

Figure 3 Differential contributions of serotonin 5-HT2A versus 5-HT2B receptors in psilocybin-induced NAc c-Fos. **A** Experimental timeline and diagram showing a coronal section with regions of interest in the NAc (*squares*). **B** Example confocal images of c-Fos, NeuN, or overlaid immunofluorescence from NAc tissue following different treatments, using a vehicle/5-HT2A/5-HT2B x saline/psilocybin design. Scale bar = 200 µm. **C** % c-Fos+ cells that were also NeuN+ across all treatment conditions, showing the majority of c-Fos+ cells were neurons under all conditions. **D** Grouped data showing c-Fos+ cell density in the NAc under different treatment conditions. **E** Grouped data showing c-Fos+ neuron (c-Fos and NeuN dual positive) density in the NAc under different treatment conditions. **F** Grouped data showing c-Fos+ non-neuron (c-Fos+ but NeuN-) density in the NAc under different treatment conditions. **D-F**, 2-way ANOVA with *Tukey*'s post hoc test. n=10-15 sections per condition. ** $p<0.01$, *** $p<0.001$, **** $p<0.0001$, ns = not significant. 2A ant = volinanserin, 2B ant = RS 127445, psi = psilocybin, veh = vehicle.

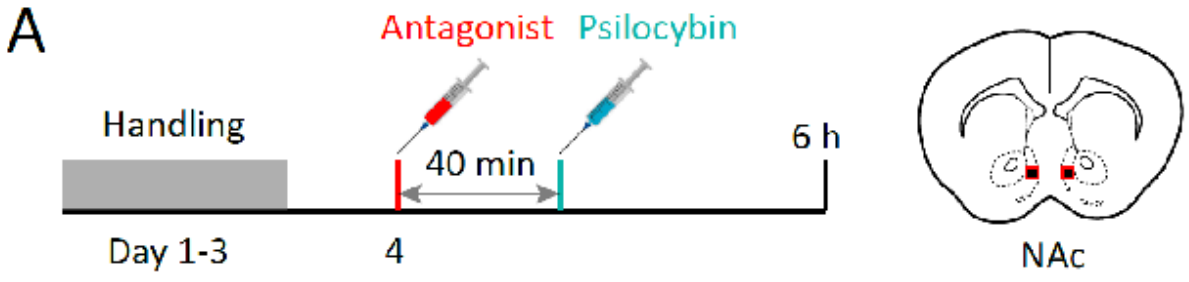

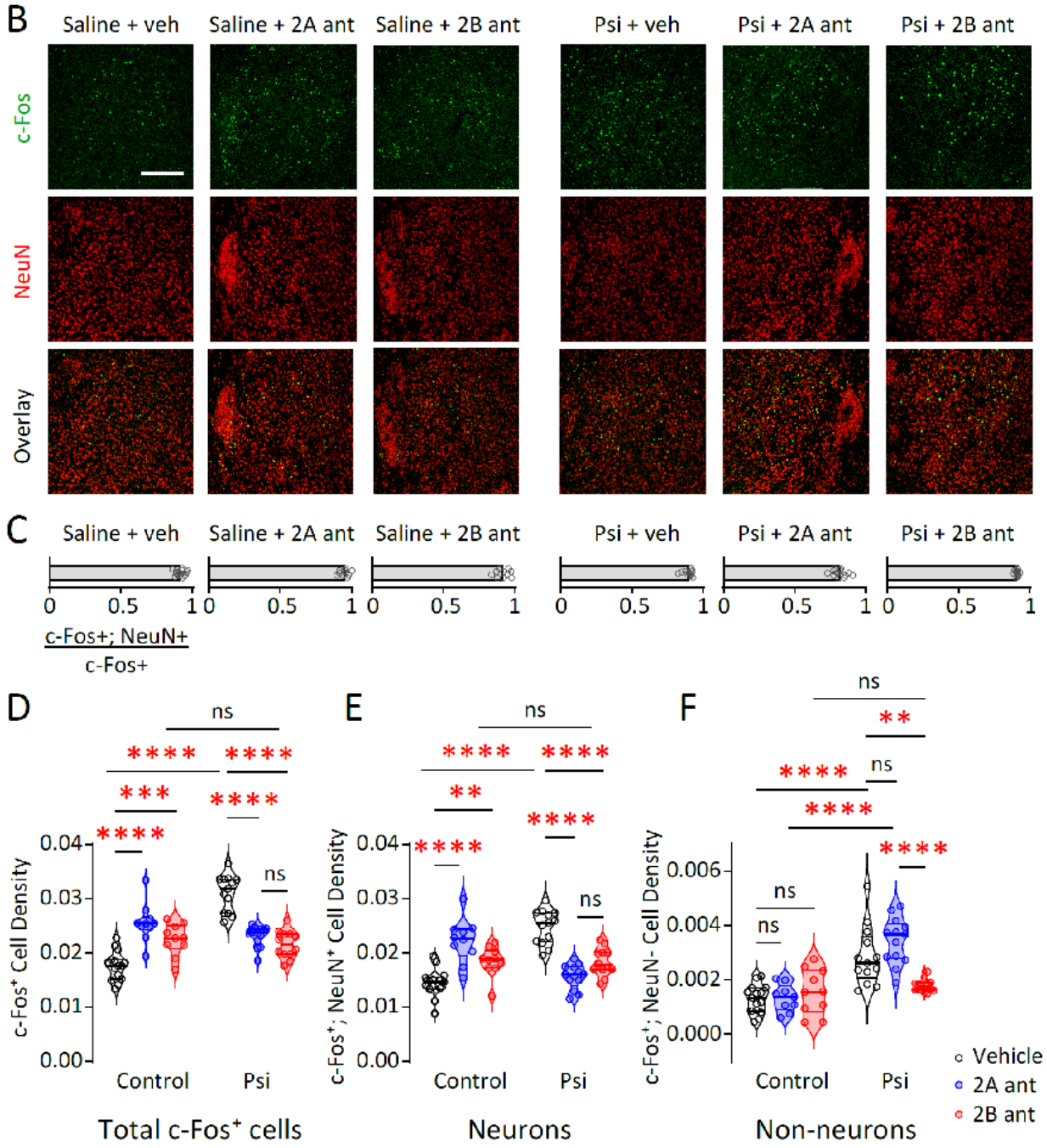

When neurons (NeuN+ cells) were examined separately, we observed similar effects of the antagonists—both attenuated the effects of psilocybin on c-Fos expression (psilocybin x antagonist interaction effect ($F(2, 67) = 56.78$, $p<0.0001$; saline versus psilocybin: $p<0.0001$,

psilocybin +vehicle versus +volinanserin: $p<0.0001$, psilocybin +vehicle versus +RS 127445: $p<0.0001$; two-way ANOVA with *Tukey*'s post-test; **Figure 3B,E**). This similarity is expected as the majority of c-Fos+ cells showed NeuN immunoreactivity (**Figure 3B,C**). On the other hand, administration of RS 127445, but not volinanserin, prevented psilocybin-induced c-Fos expression in only non-neuronal cells, suggesting 5-HT2B as the primary target for psilocybin/ psilocin to affect non-neuronal NAc cells (psilocybin x antagonist interaction effect ($F(2, 66) = 9.518$, $p<0.001$; saline versus psilocybin: $p<0.0001$, psilocybin +vehicle versus +volinanserin: $p=0.116$, psilocybin +vehicle versus +RS 127445: $p<0.01$; two-way ANOVA with *Tukey*'s post-test; **Figure 3B,F**). While both 5-HT2A and 5-HT2B are coupled with Gq-PLC-signaling, their expression exhibits region and cell type preference. Thus, two different receptor-based mechanisms underlying psilocybin's action on NAc neurons versus non-neuronal cells.

Discussion

Using computational, histochemical, and pharmacological techniques, we demonstrated the acute behavioral and delayed cellular effects of psilocybin in mice. These cell type- and receptor subtype-specific results may provide important insights for understanding the molecular and cellular underpinnings through which psychedelics impact key brain regions that regulate emotion and motivation.

The timings of psilocybin's effects

Psilocybin-induced suppression of locomotion peaked by 20 min and resolved by 1 h post-treatment (**Figure 1**), while the increase in c-Fos expression took 1.5 – 6 h (**Figure 2**). These mismatched temporal profiles suggest that psilocybin-induced activity increase in NAc cells may not contribute to psilocybin's behavioral effects. However, the following reasoning suggests otherwise. Specifically, c-Fos is an immediate early gene, whose expression is triggered

by increased cellular activity. Upon the activity increase, the transcriptional and translational machinery are activated to produce c-Fos, a process that typically peaks ~1 h following induction[19]. Thus, the increase in c-Fos expression in non-neuronal cells at 1.5 h suggests their increased activity soon after psilocybin administration. Under our experimental condition, the only external manipulation is psilocybin administration, thus serving as the most likely cause for an acute activity increase in NAc cells. We further hypothesize that NAc cells are immediately activated upon psilocybin administration and participate in the circuit mechanism to reduce locomotor activity, and the consequent c-Fos expression triggers downstream genes to produce sustained functional changes in NAc cells.

Another set of mismatched temporal profiles is that the peak expression of c-Fos in neurons was a few hours after that in non-neuronal cells (**Figure 2E**,**F**). This temporal sequence raises an intriguing possibility that the activity increase in non-neuronal cells contributes to the c-Fos expression in neurons following psilocybin. Consistent with this notion, pharmacological inhibition of 5-HT2B, which prevented psilocybin-induced c-Fos expression in non-neuronal cells, also prevented c-Fos expression in neurons following psilocybin (**Figure 3E**,**F**). While intriguing, results that support this possibility are correlative in nature. Future studies may test the causal relationship by precisely and selectively manipulating non-neuronal cells, e.g. selectively knockdown 5-HT2B in non-neuronal cells and then examine whether this manipulation affects psilocybin-induced expression of c-Fos in neurons.

Neuronal versus non-neuronal cells

About 90% of NAc neurons are the medium spiny principal neurons (MSNs), which mediate the functional output of the NAc[9]. Non-neuronal cells influence the NAc function by regulating MSNs and other neuronal cells[13]. As such, the majority of c-Fos-expressing NeuN+ cells should be MSNs. MSNs can be largely divided into two subpopulations, one expressing dopamine D1

receptors and the other expressing D2 receptors[20]. While both MSN subtypes are required for coherent performance of NAc-mediated behaviors, D1 MSNs often promote – whereas D2 MSNs inhibit – behavioral outputs[21,22]. Thus, an important future direction is to identify which subtype of MSNs is preferentially activated to express c-Fos for prolonged cellular and behavioral consequences.

Astroglia represent the majority of non-neuronal cells and outnumber neurons in most brain regions including the NAc[13]. Thus, most c-Fos-expressing non-neuronal cells may be astrocytes. Despite having large numbers, substantially fewer astrocytes exhibited psilocybin-induced c-Fos expression compared to MSNs (**Figures 2D-F**; **3E**,**F**). Nonetheless, the sparse labeling could still be impactful to the surrounding neurons, as astrocytes have a large somatic volume and extensively ramified processes, such that a single astrocyte may regulate hundreds of neurons and thousands of synapses[13]. Thus, despite the small number, astrocytes can be targeted by psilocybin to influence neuronal activities.

5-HT2A versus 5-HT2B

While 5-HT2A is the canonical receptor for initiating the hallucinogenic and psychedelic effects of psilocin, 5-HT2B is another potential target though often overlooked. In general, 5-HT2B is expressed at low levels in the mouse brain and medium levels in the human brain[23]. Nonetheless, 5-HT2B protein or mRNA is detected in several limbic brain regions including the NAc (Allen Atlas: AJ012488), shown in rodents[26]. Moreover, 5-HT2B exhibits higher binding affinity (Ki = ~4.6 nM) for psilocin than 5-HT2A (Ki = ~100 nM)[15,16]. Regarding 5-HT2B functions, in humans, mutations of 5-HT2B that impair receptor function are associated with increased impulsivity and likelihood of drug use[24,25]. Likewise, in rodents, 5-HT2B is implicated in regulating drug-reinforced behaviors[27]. Interestingly, in rodent models of depression, pharmacological inhibition of 5-HT2B prevents lysergic acid diethylamide (another

serotoninergic psychedelic)-induced anti-depressive effects *in vivo* without affecting its hallucinogenic effects[28]. These lines of evidence support the notion that 5-HT2B contributes to psilocybin's effects on regulating emotion and motivation.

Current results link 5-HT2B to the *in vivo* action of psilocybin and reveal astrocytes as a potential mediator of the psilocybin-5-HT2B-signaling in the Nac (**Figure 3**). This finding provides specific targets for future studies to test astrocytic 5-HT2B-signaling in regulating emotion and motivation.

Concluding remarks

In this study, we demonstrate that psilocybin differentially recruits 5-HT2A versus 5-HT2B to increase the activity of both neurons and non-neuronal cells in the NAc. The increased activities may not only contribute to the acute behavioral alterations following psilocybin but also trigger c-Fos-mediated transcriptional regulation to persistently change the function of NAc cells. These results depict a mechanistic standpoint, namely NAc cells, through which psilocybin influences emotion and motivation. Building upon these findings, future studies may further elucidate the differential impact of psychedelics on NAc neurons versus astrocytes, potentially guiding the development of novel therapies for emotional and motivational disorders.

References

1 Liao, C., Dua, A. N., Wojtasiewicz, C., Liston, C. & Kwan, A. C. Structural neural plasticity evoked by rapid-acting antidepressant interventions. *Nat Rev Neurosci* **26**, 101-114, doi:10.1038/s41583-024-00876-0 (2025).

2 Wong, S. *et al.* Biological markers of treatment response to serotonergic psychedelic therapies: a systematic review. *Ther Adv Psychopharmacol* **15**, 20451253251384513, doi:10.1177/20451253251384513 (2025).

3 Palhas, M., Corne, R. & Mongeau, R. Changing your mind: neuroplastic mechanisms underlying the therapeutic effect of psychedelics in depression, PTSD, and addiction. *Prog Neuropsychopharmacol Biol Psychiatry* **142**, 111533, doi:10.1016/j.pnpbp.2025.111533 (2025).

4 Kelly, D. F. *et al.* Psychedelic-Assisted Therapy and Psychedelic Science: A Review and Perspective on Opportunities in Neurosurgery and Neuro-Oncology. *Neurosurgery* **92**, 680-694, doi:10.1227/neu.0000000000002275 (2023).

5 Adeyinka, D., Forsyth, D., Currie, S. & Faraone, N. Neurobiology of psilocybin: a comprehensive overview and comparative analysis of experimental models. *Front Syst Neurosci* **19**, 1585367, doi:10.3389/fnsys.2025.1585367 (2025).

6 Cameron, L. P. *et al.* A non-hallucinogenic psychedelic analogue with therapeutic potential. *Nature* **589**, 474-479, doi:10.1038/s41586-020-3008-z (2021).

7 Hyman, S. E. & Malenka, R. C. Addiction and the brain: the neurobiology of compulsion and its persistence. *Nat Rev Neurosci* **2**, 695-703, doi:10.1038/35094560 (2001).

8 Cox, J. & Witten, I. B. Striatal circuits for reward learning and decision-making. *Nat Rev Neurosci* **20**, 482-494, doi:10.1038/s41583-019-0189-2 (2019).

9 Meredith, G. E., Baldo, B. A., Andrezjewski, M. E. & Kelley, A. E. The structural basis for mapping behavior onto the ventral striatum and its subdivisions. *Brain Struct Funct* **213**, 17-27, doi:10.1007/s00429-008-0175-3 (2008).

10 Mogenson, G. J., Yang, C. R. & Yim, C. Y. Influence of dopamine on limbic inputs to the nucleus accumbens. *Ann N Y Acad Sci* **537**, 86-100, doi:10.1111/j.1749-6632.1988.tb42098.x (1988).

11 Zinsmaier, A. K., Nestler, E. J. & Dong, Y. Astrocytic G Protein-Coupled Receptors in Drug Addiction. *Engineering (Beijing)* **44**, 256-265, doi:10.1016/j.eng.2024.12.016 (2025).

12 Khakh, B. S. On astrocyte-neuron interactions: Broad insights from the striatum. *Neuron* **113**, 3079-3107, doi:10.1016/j.neuron.2025.08.009 (2025).

13 Wang, J. *et al.* Astrocytes in cocaine addiction and beyond. *Mol Psychiatry* **27**, 652-668, doi:10.1038/s41380-021-01080-7 (2022).

14 Kwan, A. C., Olson, D. E., Preller, K. H. & Roth, B. L. The neural basis of psychedelic action. *Nat Neurosci* **25**, 1407-1419, doi:10.1038/s41593-022-01177-4 (2022).

15 Rickli, A., Moning, O. D., Hoener, M. C. & Liechti, M. E. Receptor interaction profiles of novel psychoactive tryptamines compared with classic hallucinogens. *Eur Neuropsychopharmacol* **26**, 1327-1337, doi:10.1016/j.euroneuro.2016.05.001 (2016).

16 Halberstadt, A. L. & Geyer, M. A. Multiple receptors contribute to the behavioral effects of indoleamine hallucinogens. *Neuropharmacology* **61**, 364-381, doi:10.1016/j.neuropharm.2011.01.017 (2011).

17 Peng, L., Song, D., Li, B. & Verkhratsky, A. Astroglial 5-HT(2B) receptor in mood disorders. *Expert Rev Neurother* **18**, 435-442, doi:10.1080/14737175.2018.1458612 (2018).

18 Lu, O. D. *et al.* A multi-institutional investigation of psilocybin's effects on mouse behavior. *bioRxiv*, doi:10.1101/2025.04.08.647810 (2025).

19 Whitaker, L. R. & Hope, B. T. Chasing the addicted engram: identifying functional alterations in Fos-expressing neuronal ensembles that mediate drug-related learned behavior. *Learn Mem* **25**, 455-460, doi:10.1101/lm.046698.117 (2018).

20 Gong, S. *et al.* A gene expression atlas of the central nervous system based on bacterial artificial chromosomes. *Nature* **425**, 917-925, doi:10.1038/nature02033 (2003).

21 Lobo, M. K. & Nestler, E. J. The striatal balancing act in drug addiction: distinct roles of direct and indirect pathway medium spiny neurons. *Front Neuroanat* **5**, 41, doi:10.3389/fnana.2011.00041 (2011).

22 Kupchik, Y. M. *et al.* Coding the direct/indirect pathways by D1 and D2 receptors is not valid for accumbens projections. *Nat Neurosci* **18**, 1230-1232, doi:10.1038/nn.4068 (2015).

23 Acevedo-Triana, C. A., Leon, L. A. & Cardenas, F. P. Comparing the Expression of Genes Related to Serotonin (5-HT) in C57BL/6J Mice and Humans Based on Data Available at the Allen Mouse Brain Atlas and Allen Human Brain Atlas. *Neurol Res Int* **2017**, 7138926, doi:10.1155/2017/7138926 (2017).

24 Lin, Z., Walther, D., Yu, X. Y., Drgon, T. & Uhl, G. R. The human serotonin receptor 2B: coding region polymorphisms and association with vulnerability to illegal drug abuse. *Pharmacogenetics* **14**, 805-811, doi:10.1097/00008571-200412000-00003 (2004).

25 Bevilacqua, L. *et al.* A population-specific HTR2B stop codon predisposes to severe impulsivity. *Nature* **468**, 1061-1066, doi:10.1038/nature09629 (2010).

26 Duxon, M. S. *et al.* Evidence for expression of the 5-hydroxytryptamine-2B receptor protein in the rat central nervous system. *Neuroscience* **76**, 323-329, doi:10.1016/s0306-4522(96)00480-0 (1997).

27 Doly, S. *et al.* Role of serotonin via 5-HT2B receptors in the reinforcing effects of MDMA in mice. *PLoS One* **4**, e7952, doi:10.1371/journal.pone.0007952 (2009).

28 Bouloufa, A. *et al.* LSD's rapid antidepressant effects are modulated by 5-HT(2B) receptors. *Biomed Pharmacother* **190**, 118348, doi:10.1016/j.biopha.2025.118348 (2025).